Entanglement of Embedded Graphs

Toen Castle, Myfanwy E. Evans and Stephen T. Hyde

Applied Mathematics Dept., Research School of Physics, Australian National University, Canberra, 0200, Australia

(Received December 1, 2010)

We discuss the identification of untangled graph embeddings for finite planar and non-planar graphs as well as infinite crystallographic nets. Two parallel approaches are discussed: explicit 3-space embeddings and reticulations of 2-manifolds. 2D and 3D energies are proposed that allow ranking of (un)tangled embedding graphs.

§1. Introduction

Graphs, G are topological objects, composed of a collection of vertices, v_i ($i \in \{1, N\}$) and edges, e_j, associated with vertex pairs, $e_j(v_k, v_l)$. For simplicity, assume that G is *simple* (i.e. for any $\{k, l\}$, the number of associated edges is at most one). We are interested in embeddings of topological graphs in euclidean 3-space, $\mathcal{G}$, motivated by the plethora of three-dimensional chemical structures, which can be idealised as embedded graphs. The vertices and edges of these graphs correspond to atoms and chemical bonds in covalent crystals or organic molecules; in the case of supra-molecular materials such as metal-organic frameworks (MOFs) or DNA assemblies) these coincide with molecular groups and polymeric ligands or H-bonds respectively. We are interested in the effects of the graph embedding on the behaviour of the material.

These issues are relevant to the physical properties of materials. For example, the hardness of physical glasses can be correlated with the rigidity in the resulting bonding network, and is therefore critically dependent on the topology of the glass network.[22] The viscosity of polymers in solution is intimately associated with the entanglement of the polymer chains within the solution.[10] Here we explore aspects of ambient isotopy of graph embeddings. Define all embeddings $\mathcal{G}$ of a graph G that share a common ambient isotopy as equivalent *isotopes*. Distinct isotopes — which are not ambient isotopic — differ in the relative *entanglement* of graph edges. Definition of entanglement requires elucidation of an unentangled 'ground state' isotope, $\mathcal{G}_0$, of a graph. We propose a definition for $\mathcal{G}_0$ for generic G, including infinite graphs, later in this paper. For now, we assume G is 3-connected and planar (and simple), so that it is a *polyhedral graph*.[11] In this case, $\mathcal{G}_0$ necessarily embeds in the sphere ($\mathbb{S}^2$) without edge crossings. This is also sufficient to characterise $\mathcal{G}_0$, since Whitney's theorem ensures that the 2-cell embedding of $\mathcal{G}$ into $\mathbb{S}^2$ — the isotope $\mathcal{G}_0$ — is unique.[24]

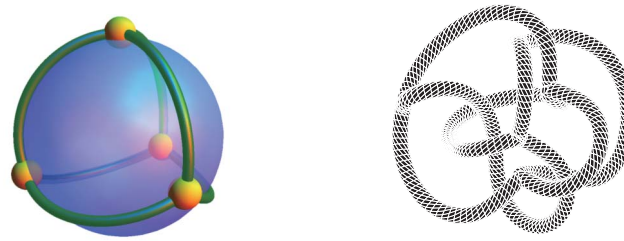

(a) (b)

Fig. 1. (a) The untangled isotope of the tetrahedral graph, K_4 (reticulating a sphere). (b) A tangled isotope of K_4 that contains neither knots nor links.

§2. Graph entanglement compared with knotting

If $\mathcal{G}{=}\mathcal{G}_0$, it can be embedded in $\mathbb{S}^2$, so it cannot contain knots and/or links. Therefore, if the isotope $\mathcal{G}$ contains a subgraph that form knots and/or links, $\mathcal{G}$ is entangled. Knots (and links) are non-trivial embeddings of one (or more) cycles within G, so the underlying sub-graph responsible for this class of entanglement consists of graph cycles homeomorphic to S^1.

Note however, that the absence of knots and/or links is not sufficient to force $\mathcal{G}$ to be untangled. Consider for example, the untangled embedding of $G = K_4$ illustrated in Fig. 1(a). The embedding of K_4 shown in Fig. 1(b) is evidently tangled, since it cannot be drawn in the plane, yet it is also free of knots and/or links. We call this mode of entanglement a *ravel*.[4] This example demonstrates the distinction between "knotted" and tangled graphs.*)

In contrast to knots and links, that are formed by graph minors homeomorphic to $\mathbb{S}^1$, the graph fragments that induces entanglements of the type shown in Fig. 1 are stars of edges common to a single vertex of the graph. By definition, all *ravels* are associated with the star of edges sharing a single vertex.[4] 'Star' subgraphs therefore offer a second motif that can induce tangled embeddings of graphs. Interestingly, the first examples of a molecule whose bonding network contains a ravel as a proper subgraph has been reported recently.[19]

§3. Simple entanglements of polyhedral graphs: toroidal embeddings

What are the simplest examples of tangled polyhedral graphs? Since untangled polyhedral graphs have 2-cell embeddings in the (genus zero) sphere, $\mathbb{S}^2$, simple tangled embeddings embed in the (genus one) torus rather than $\mathbb{S}^2$. (We assume that the torus itself is embedded in 3-space in the standard manner, rather than a more exotic twisted or knotted embedding). We conjecture that all isotopes ($\mathcal{G}_1$) of G that embed in the torus contain knots and/or links. Certainly, 2-cell embeddings

*) This possibility has been recognised already by graph theorists. For example, the isotope of K_4 in Fig. 1(b) contains a graph-minor equivalent to Kinoshita's $\theta-$graph embedding.[16] Kawauchi introduced 'minimally knotted' embedded graphs.[15] These are a subset of ravels, that we call 'fragile' ravels.[4]

of ravels, or embedded graphs containing ravels as minors, are only possible on manifolds whose genera exceed one. We assume that other tangled embeddings, which are knot-free, but tangled due to (as yet unclasssified) tangled graph motifs other than knots, links or ravels, also embed in orientable manifolds whose genera exceed one. It follows from this conjecture that *all* toroidal embeddings of polyhedral graphs are chiral.[2] (Note that this result is specific to polyhedral graphs; examples of achiral toroidal embeddings of planar 2-connected and planar multigraphs exist.)

Ranking of the toroidal embeddings $\mathcal{G}_1$ of a polyhedral graph can be done in various ways. One route, that makes explicit use of the embedding in euclidean 3-space ($\mathbb{E}^3$) is to extend the concept of a 'tight knot' embedding[1] as follows. A tight embedding of an isotope is one that minimises the ratio of total length of edges L in the embedding $\mathcal{G}_1$ divided by a steric diameter of the edges, D. No overlap or crossing of edges is allowed during the tightening procedure, conserving the ambient isotopy of the isotope throughout the process. A numerical algorithm that estimates the minimiser of this ratio has been implemented for graphs.[7] We then rank toroidal embeddings ordered by the 3D energy function:

$$E_{3d}(\mathcal{G}_1) = \frac{L}{D}.$$

Another ranking emerges from the 2-cell embedding in the torus, and makes no explicit reference to the 3-space embedding. Rather, we form a barycentric placement of the 2-periodic net of edges that arises from the 2-cell embedding in the torus lifted to the universal cover ($\mathbb{E}^2$).[6] Barycentric placement guarantees that the sum Σl_i^2 over all edge length l_i, is minimised.[6] That calculation can be done readily using the *GAVROG* package, available on-line,[9] giving embedding coordinates of all graph vertices within a single 'unit cell' of the 2-periodic pattern in $\mathbb{E}^2$, formed in the universal cover. Those coordinates are crystallographic coordinates, which correspond to euclidean cartesian coordinates when the unit cell is a euclidean square, with orthogonal lattice vectors $(1, 0)$ and $(0, 1)$. Barycentric placement is however conserved by all affine transformations of the square unit cell to a rhombus with lattice vectors (q, r) and (s, t), where $q, r, s, t \in \mathbb{Z}$. The values of q, r, s, t determine the homotopy types of all cycles of $\mathcal{G}_1$ in the torus.

An explicit tangled polyhedral isotope $\mathcal{G}_1$, is formed as follows. First, find all 2-cell embeddings of the graph G in the torus, forming toroidal graphs $\mathcal{G}_1$. Next, form planar graphs from $\mathcal{G}_1$ by pulling back these toroidal graphs to their universal covers, giving 2-periodic nets g_{2d} in $\mathbb{E}^2$. Relax each g_{2d} to form a barycentric embedding, giving crystallographic coordinates (x, y) for each vertex and then form an explicit 2-periodic embedding of the net in $\mathbb{E}^2$ by choosing lattice vectors (q, r) and (s, t) (with $|qt - rs| = 1$) with respect to the crystallographic basis.

Explicit (cartesian) vertex coordinates can then be determined from the formula

$$\begin{bmatrix} x \\ y \end{bmatrix}_{new} = \begin{bmatrix} q & r \\ s & t \end{bmatrix} \begin{bmatrix} x \\ y \end{bmatrix}.$$

One degree of freedom remains that does not affect the homotopy type of the embedding: a scaling factor that preserves unit cell area, $\alpha \in \mathbb{R}^+$, giving vertex

coordinates: $(x', y') = (\alpha x, \alpha^{-1} y)$, from which edge lengths (l_i) are calculated with the usual euclidean metric. The value of α is chosen to give an absolute minimum of Σl_i^2.

The 3-space embedding of $\mathcal{G}_1$ forms by pulling back the resulting graph to an embedding in the torus, then regluing the unit cell according to its pair of lattice vectors. Embed the torus in $\mathbb{E}^3$ in the standard manner, and lastly, dissolve the torus, leaving the graph embedded in 3-space. In summary, the data $[g_{2d}, q, r, s, t]$ maps (many-to-one) to an embedding $\mathcal{G}_1$.

Toroidal embeddings are then ranked by a (2D) energy function:

$$E_{2d}(\mathcal{G}_1) = \Sigma_i l_i^2,$$

where l_i denotes one of the edge lengths.

These alternative 2D and 3D approaches to ranking of tangled polyhedral isotopes are best illustrated by an example. Let G be the graph given by edges of a cube, Q, containing 8 vertices of degree-3. Four non-homeomorphic 2-periodic planar nets g_{2d}^{Q} can be pulled back to the torus to give toroidal cube embeddings, $\mathcal{Q}_1$. One of those is the net of edges formed by the tessellation of $\mathbb{E}^2$ by hexagons, with Schläfli symbol $\{6, 3\}$. Barycentric relaxation of this net gives a 2-periodic pattern, for which a square-shaped unit cell of unit area, bounded by lattice vectors $(1, 0)$ and $(0, 1)$ and containing a single copy of each cube vertex can be drawn (Fig. 2(a)). If alternative lattice vectors $(1, 2)$ and $(1, 0)$ are chosen as a basis for the fundamental group of a torus, the universal cover wraps up to form the isotope in the torus illustrated in Fig. 2(b), that embeds in 3-space to give the $\mathcal{Q}_1$ shown in Fig. 2(c), referred to elsewhere as a type-B toroidal cube.[3),12)] The presence of a $(2, 4)$ link in $\mathcal{Q}_1$ imposes non-planarity on the embedding, proving the entanglement of this isotope.[12)] The energy, E_{2d}, of this embedding $\mathcal{G}_1$ of the isotope $\mathcal{Q}_1$ assumes a value of 2.31 with alpha=0.658 (when $\alpha = 1.52$). (It turns out that this $\mathcal{G}_1$ is not the least energy one for this isotope. An alternative $[g_{2d}, q, r, s, t]$ exists, which pulls back to an identical $\mathcal{G}_1$ with a smaller value of E_{2d}, 2.20[3)]).

The isotope $\mathcal{Q}_1$ can be tightened in euclidean 3-space to minimise the magnitude of E_{3d}. The 3D tightening process results in the embedding shown in Fig. 2(d), for which $E_{3d} = 24.63$.

These complementary two- and three-dimensional approaches give a ranking of the least tangled isotopes $\mathcal{G}_1$ of the graph Q tabulated in Table I. The two- and three-dimensional approaches give similar, though not identical, rankings; a result which suggests that both energy functions are useful. The exact calculations (and relative simplicity) of the two-dimensional approach are helpful though they make no reference to 3-space embeddings. In contrast, the tightening algorithm affords 3-space embeddings, despite the numerical uncertainty surrounding the tightening algorithm required for these calculations. It is likely that tight embeddings of generic knotted graphs share the non-uniqueness inherent in some tight link embeddings.[1)] However, numerical relaxation of a number of examples of polyhedral isotopes reveal convergence to a common embedding for each isotope, regardless of the choice of initial embedding. We are therefore optimistic that this tightening algorithm offers a useful structural signature of many isotopes, assuming a unique tight embedding.

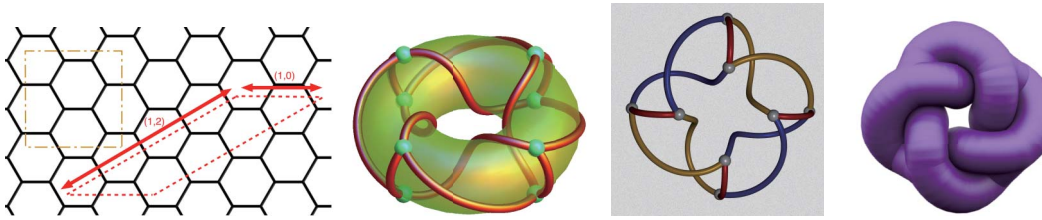

(a) (b) (c) (d)

Fig. 2. (a) A 2-periodic graph that is a universal cover of the graph of cube edges reticulating a torus, g^{Q}_{2d}. A unit cell (dashed rectangle) containing 8 distinct vertices of degree 3 is shown. A skew unit cell made of $(1,0)$ and $(1,2)$ lattice vectors of the simpler cell is marked by the dotted rhombus. (b) If the $(1,0)$ and $(1,2)$ lattice vectors are adopted as generators of the fundamental group of a torus, and the patch is glued to form a torus, a toroidal reticulation is formed. (c) The embedding in 3-space of this reticulation is a B-type tangled cube graph, $\mathcal{Q}_1$. (d) This isotope can be annealed in 3D space to form a tight configuration, that minimises the ratio of edge length to diameter.

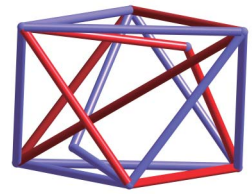

Fig. 3. (color online) The untangled K_6 isotope. Note the presence of a link, marked by the threaded (red) cycles.

§4. Entanglements of non-planar finite graphs: untangled embeddings

So far, the embedded graphs have been limited to polyhedral examples. Since these graphs are topologically planar, their untangled state is particularly simple, corresponding to the (unique) isotope whose minimal embedding is in the (genus-zero) sphere. By extension of this 2D embedding principle, we demand that untangled embeddings of *nonplanar* graphs are isotopes whose 2-cell embeddings reticulate (oriented) 2-manifolds of minimal genus. Thus, for example, the K_6 graph — which cannot be embedded in $\mathbb{S}^2$, can be embedded in the (genus-one) torus in four ways.[18] The resulting universal covers are four distinct 2-periodic graphs, g_{2d}, however all of these embed in the torus to form equivalent isotopes in $\mathbb{E}^3$. We therefore choose this as the untangled isotope of K_6. This definition of the untangled state is at first glance less than satisfactory, given that the toroidal embeddings contain a link (Fig. 3). However, it is known that any embedding of K_6 results in at least a single link.[5] Our untangled isotope can therefore never be embedded with less entanglement. Here too we distinguish between entanglement and knottedness: just as tangled isotopes need not be knotted, knotted (or linked) isotopes need not be tangled.

In general, nonplanar graphs $\mathcal{G}$ will have many isotopes whose 2-cell embeddings

Table I. Simpler tangled toroidal cube isotopes, $\mathcal{Q}_1$, formed reticulations of 2-periodic graphs ($g^{\mathcal{Q}}_{2d}$) in the torus, mapping particular lattice vectors (forming the dotted rhombi in the $g^{\mathcal{Q}}_{2d}$ images) onto the pair of generators of the torus' fundamental group. The resulting isotopes are annealed in 3-space to form 'tight' configurations illustrated in the rightmost column. (To aid visualisation, the edges' diameter has been reduced from their optimal tight values.) Relative 2D and 3D energies (E_{2d} and E_{3d}) are listed; their values are calculated from formulae given in the main text.

$g^{\mathcal{Q}}_{2d}$	$\mathcal{Q}_1$	E_{2d}	tight 3-space embedding	E_{3d}
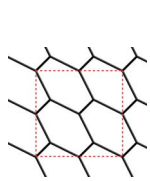	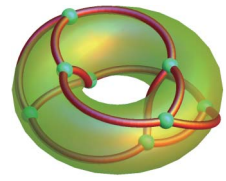	1.33	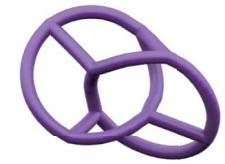	16.97
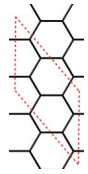	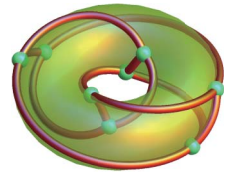	1.76		21.04
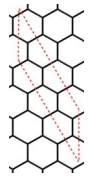	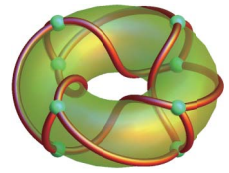	2.20	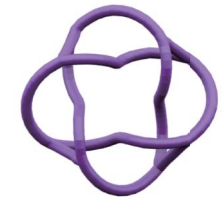	24.63
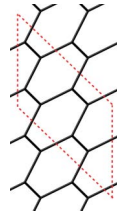	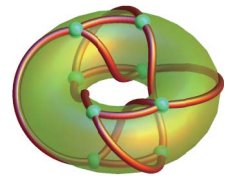	2.31	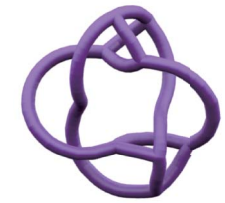	25.21
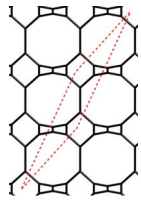	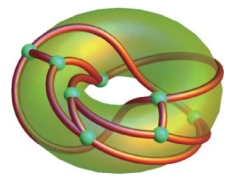	2.82		23.77

form in the simplest possible 2-manifolds, with minimal genus. In those cases, we must delve further to select a single untangled isotope. By analogy with the simpler tangled examples considered above, we may choose the untangled isotope by analysis of its 2-periodic universal cover (via E_{2d}) or the energy of its tightest configuration in $\mathbb{E}^3$, via E_{3d}.

Within our 2D view, we select the isotope with the shortest edge length within the universal cover derived from its reticulation of the minimal-genus orientable 2D manifold. Note that in general, since that manifold is a multi-handled torus with genus (γ) exceeding one, the graph that emerges within the universal cover, g_{2d}, is an infinite (2γ-)periodic pattern. In that case, the image of a single copy of the manifold (in the hyperbolic plane, $\mathbb{H}^2$) is a 4γ-gon, whose area is constant, regardless of its specific shape. Barycentric relaxation of g_{2d}, minimising $\Sigma_i l_i^2$, is mathematically well-defined,[23] though explicit implementation is more delicate than for the case where $\gamma = 1$ (when g_{2d} is a 2-periodic pattern in $\mathbb{E}^2$), since integer arithmetic — which allows exact calculation of barycentric embeddings within $\mathbb{E}^2$,[6] — is no longer possible, due to the non-euclidean nature of $\mathbb{H}^2$.

Alternatively, the untangled isotope, $\mathcal{G}_0$, may be defined as that which minimises E_{3d} among all isotopes of $\mathcal{G}$ that embed in the manifold of minimal genus.

In general, the two- and three-dimensional approaches may not give the same isotope as the untangled case, just as the ranking of simpler tanged cube isotopes may differ (*cf.* Table I). Further exploration of the differences between these alternatives is needed.

§5. Untangled embeddings of non-planar infinite crystallographic graphs

Suppose we allow $\mathcal{G}$ to be infinite, and *crystallographic*, in the sense that the graph G_{cryst} can be embedded in $\mathbb{E}^3$ as a three-periodic crystalline pattern (a graph theoretic definition can be found in Ref. 17). Generalisation of the numerical algorithm to deduce tight embeddings of finite graphs to crystallographic graphs is feasible, and relative energies of various isotopes of $\mathcal{G}_{cryst}$ within the 3D view, E_{3d}, can be readily (if numerically slowly) estimated.[8] Since the graphs are infinite, the numerator of E_{3d} counts only edge lengths within a crystallographic unit cell of the pattern. We propose that untangled isotopes of three-periodic crystallographic graphs are — within this 3D view — those that globally minimise E_{3d} among all possible isotopes. It is very likely that those are equivalent isotopes to the embedding formed by the barycentric embedding of $\mathcal{G}_{cryst}$, assuming this embedding avoids coincident vertices and/or edge crossings. For simpler three-periodic crystallographic nets, tight embeddings are identical to barycentric configurations, whose embedding is chosen to realise all graph isometries as explicit geometric isometries in $\mathbb{E}^3$ (accessible via 9) and explored in 6)). In other cases (where, for example, the graph contains more than one distinct edge type), tight and barycentric embeddings may not coincide. Further, collisions of edges and/or vertices can (occasionally) arise in barycentric embeddings.[6] In those cases the barycentric embedding has coincident vertices, or distinct edges cross through each other. Despite collisions, these embeddings too can be tightened numerically to form collision-free embeddings, allowing determination of E_{3d} for various isotopes. We note that such examples may lead to more than one untangled isotope, since degeneracy of E_{3d} for distinct isotopes is possible in those cases.

Consider lastly the analysis of the untangled isotope of $\mathcal{G}_{cryst}$ within our 2D

approach. In that case, the minimal genus of a 2-manifold that can be reticulated by G is unbounded. Here too, the universal cover is $\mathbb{H}^2$. Computation of the 2D energy function, E_{2d}, is delicate, since the number of edges in the graph g_{2d} diverges, as does the area A associated with a single copy of the manifold. However, since G is crystallographic, g_{2d} contains isometries, and we can compute E_{2d} as follows, provided g_{2d} forms the edges of a tessellation of $\mathbb{H}^2$ with finite polygonal tiles. First, note that Euler's Theorem (which relates the Euler characteristic χ to the number of vertices V, edges E and faces F) can be used to deduce the area per vertex, $\frac{A}{V}$, of g_{2d} in $\mathbb{H}^2$. This area is related to the (average) degree of each vertex of g_{2d}, z and the (average) number of vertices in each fundamental cycle of g_{2d}, n:

$$\frac{\chi}{V} = 1 - \frac{E}{V} + \frac{F}{V} = 1 - \frac{z}{2} + \frac{z}{n}.$$

Therefore

$$\frac{\chi}{V} = 1 + \frac{z(2-n)}{2n}.$$

From the global Gauss-Bonnet theorem, $2\pi\chi = KA$, where K is the Gaussian curvature, namely -1 in $\mathbb{H}^2$, so that

$$\frac{A}{V} = 2\pi\left[\frac{z(n-2)}{2n} - 1\right].$$

The edge length per vertex in the hyperbolic graph embedding g_{2d} depends on the geometry of the embedding. If we assume that the g_{2d} graph has Schläfli symbol $\{n, z\}$, and embeds with maximum symmetry (as a 'regular' embedding, with symmetrically identical vertices, edges and faces), its asymmetric domain corresponds to a single domain of a $\star 2nz$ orbifold. In that case, hyperbolic trigonometry implies that the edge length l_i in g_{2d} is equal to $2\arccos h\left[\cot(\frac{\pi}{n})\cot(\frac{\pi}{z})\right]$, so that

$$E_{2d} := \frac{\Sigma_i l_i^2}{A} = \frac{z(\arccos h\left[\cot(\frac{\pi}{n})\cot(\frac{\pi}{z})\right])^2}{2\pi\left[\frac{z(n-2)}{2n} - 1\right]}.$$

Given the barycentric nature of the regular $\{n, z\}$ tiling in any 2D space, we conjecture that this formula offers a lower bound of E_{2d} for three-periodic crystallographic graphs, $\mathcal{G}_{cryst}$. Since z is equal to the degree of $\mathcal{G}_{cryst}$, only the value of n remains to be determined from the 2-manifold embedding.

Two examples illustrate these 3D and 2D approaches for crystallographic graphs. Consider first the net of edges of a tessellation of $\mathbb{E}^3$ by cubes, known to crystal chemists as **pcu**,[20] illustrated in Fig. 4(a). This embedding is barycentric and is equivalent to the tight embedding, from which we deduce a 3D energy $E_{3d} \approx 3.0005$ for the untangled cube isotope, $\mathcal{G}_0$. Since this embedding is barycentric, it qualifies as the untangled isotope of **pcu** according to the 3D definitions proposed above.

The equivalent isotope emerges by reticulating the infinite-handled 2-manifold (Fig. 4(b)), which can be smoothed in $\mathbb{E}^3$ to form the triply-periodic minimal surface known as the P-surface[13),21] (Fig. 4(c)). The universal cover of the reticulation of this manifold by the **pcu** net is the regular $\{4, 6\}$ tiling of $\mathbb{H}^2$ (Fig. 4(d)), which has

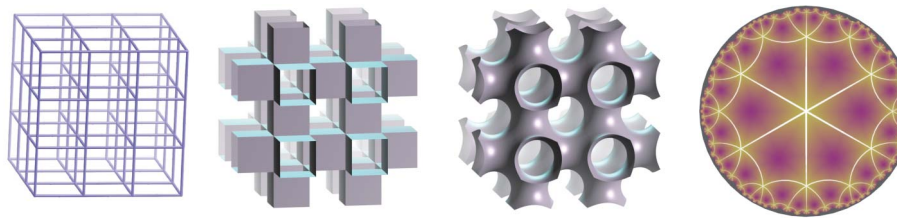

(a) (b) (c) (d)

Fig. 4. (a) The untangled isotope of the **pcu** crystallographic net. (b) A facetted infinite-genus manifold whose edges are those of **pcu**. (c) A smoothed version of (b), corresponding to the three-periodic P-surface. (d) The universal cover of the $\{4,6\}$ graph (g_{2d}) drawn within the Poincaré model of the hyperbolic plane.

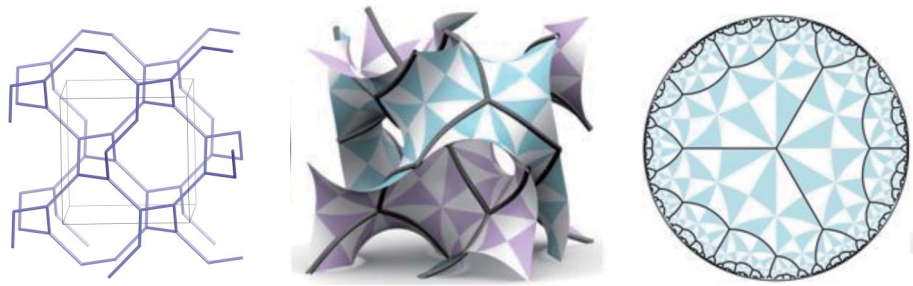

(a) (b) (c)

Fig. 5. (a) The untangled isotope of the **srs** net. (b) Reticulation on the gyroid minimal surface by a pair of these isotopes. (c) Universal cover (in $\mathbb{H}^2$) of the reticulation in (b).

symmetry ⋆246. From the formula above, it follows that when $\mathcal{G}_{cryst} = \mathbf{pcu}$, and it is embedded in the P-surface with this symmetry, $E_{2d} = \frac{6(\text{arccosh}(\sqrt{3}))^2}{\pi} \approx 2.509$.

A second example of a crystallographic graph is the degree-3 graph known as **srs**,[20] one of whose isotopes is illustrated in Fig. 5(a). This isotope is realised in a barycentric embedding; it therefore qualifies as the untangled isotope, $\mathcal{G}_0$ of **srs**. The barycentric embedding with cubic symmetry is already tight, and gives a value of $E_{3d} \approx 11.883$.

The 2D description of this isotope of **srs** is more complex than for **pcu**. Since the smallest cycles in the **srs** graph are decagons, n in g_{2d} must exceed 9. Assume, for now that g_{2d} is a regular $\{10,3\}$ tiling of $\mathbb{H}^2$. Applying the formula above gives $E_{2d} = \frac{15\left(\text{arccosh}\left[\sqrt{\frac{5+2\sqrt{5}}{3}}\right]\right)^2}{2\pi} \approx 3.309$. However, a regular $\{10,3\}$ graph cannot be formed on a 2-manifold embedded in $\mathbb{E}^3$ (since a manifold with ⋆23(10) symmetry is incommensurate with euclidean space). To date, the best reticulation we have found is a regular degree-three tree with edge length $\arccos h(3)$ and symmetry ⋆2223, that maps onto the gyroid triply-periodic minimal surface without distortion to form (a pair of) untangled **srs** net(s), as illustrated in Fig. 5.[14] Since the area per ⋆2223 fundamental domain is $\frac{\pi}{3}$ and each domain contains a half-edge, $E_{2d} = \frac{3(\text{arccosh}(3))^2}{\pi} \approx$

2.967.

Acknowledgements

STH is grateful to the organisers of the Kyoto meeting. We thank Gerd Schröder-Turk and Stuart Ramsden for generating the images in Figs. 2(c) and 4.

References

1) J. Cantarella, R. B. Kusner and J. M. Sullivan, Invent. Math. **150** (2002), 257.
2) T. Castle, M. E. Evans and S. T. Hyde, New J. Chem. **33** (2009), 2107.
3) T. Castle, V. Robins and S. T. Hyde, "Toroidal entangled polyhedral graphs: Tetrahedra, octahedra and cubes", in preparation.
4) T. Castle, M. E. Evans and S. T. Hyde, New J. Chem. **32** (2008), 1484.
5) J. H. Conway and C. M. Gordon, J. Graph Th. **7** (1983), 445.
6) O. Delgado-Friedrichs and M. O'Keeffe, Acta Cryst. A **59** (2003), 351.
7) M. Evans, V. Robins and S. T. Hyde, "Tight embeddings of periodic nets", in preparation.
8) M. Evans, "Three-dimensional entanglement: knots, knits and nets", PhD thesis, (Australian National University, 2011).
9) Olaf Delgado Friedrichs, The Gavrog Project, `http://www.gavrog.org/`
10) P. G. De Gennes, Macromolecules **9** (1976), 587.
11) B. Grünbaum, Discrete Math. **307** (2007), 445.
12) S. T. Hyde and G. Schröder-Turk, Acta Cryst. A **63** (2007), 186.
13) S. T. Hyde, O. Delgado-Friedrichs, S. J. Ramsden and V. Robins, Solid State Sciences **8** (2006), 740.
14) S. T. Hyde and C. Oguey, Eur. Phys. J. B **16** (2000), 613.
15) L. Kawauchi, "Hyperbolic imitation of 3-manifolds" (1987).
16) S. Kinoshita, Pac. J. Math. **42** (1972), 89.
17) W. E. Klee, Cryst. Res. Technol. **39** (2004), 959.
18) William Kocay, K6 torus embeddings (2006), `http://bkocay.cs.umanitoba.ca/g&g/K6Torus.html`
19) F. Li, J. K. Clegg, L. F. Lindoy, R. B. Macquart and G. V. Meehan, Nature Comm. **2** (2011), 205.
20) M. OKeeffe, M. A. Peskov, S. J. Ramsden and O. M. Yaghi, Acc. Chem. Res. **41** (2008), 1782.
21) V. Robins, S. J. Ramsden and S. T. Hyde, Acta Cryst A **39** (2009), 365.
22) M. M. Smedskjaer, J. C. Mauro and Y. Yue, Phys. Rev. Lett. **105** (2010), 115503.
23) A. A. Ungar, *Hyperbolic Triangle Centers* (Springer, 2010).
24) H. Whitney, Amer. Math. J. **55** (1933), 245.